Cellular Physiology and Biochemistry

Cell Physiol Biochem 2018;46:815-828
DOI: 10.1159/000488739
Published online: April 06, 2018
Accepted: February 08, 2018

Original Paper

Effects of Long Non-Coding RNA LINC00963 on Renal Interstitial Fibrosis and Oxidative Stress of Rats with Chronic Renal Failure via the Foxo Signaling Pathway

Wen Chen Lei Zhang Zhong-Qi Zhou Yue-Qin Ren Li-Na Sun Yu-Lin Man Zhong-Wei Ma Zhi-Kui Wang

Department of Nephrology, Linyi People's Hospital, Linyi, P.R. China

Key Words
Long intergenic non-coding RNA 00963 • Chronic renal failure • FoxO signaling pathway • Renal interstitial • Oxidative stress

Abstract
Background/Aims: Chronic renal failure (CRF) is usually associated with chronic diseases such as congestive heart failure and diabetes mellitus, the prevalence of which is increased with age. This study is designed to investigate the role of long intergenic non-coding RNA (lincRNA) LINC00963 in renal interstitial fibrosis (RIF) and oxidative stress (OS) of CRF via the forkhead box O (FoxO) signaling pathway. ***Methods:*** Microarray data and annotated probe files related to CRF were downloaded by retrieving Gene Expression Omnibus (GEO) database to screen differentially expressed lncRNA. Multi Experiment Matrix (MEM) website and dual-luciferase reporter gene assay were used to predict and verify the target gene of LINC00963, and Kyoto Encyclopedia of Genes and Genomes (KEGG) enrichment analysis to identify the major signaling pathways involved. A total of 60 Wistar male rats were randomly selected and divided into the sham (n = 10) and model (n = 50) groups. Five rats in the sham group and thirty rats in the model group were sub-categorized into the control, blank, negative control (NC), LINC00963 vector, si-LINC00963, si-FoxO3, and si-LINC00963 + si-FoxO3 groups (n = 5). Reverse transcription quantitative polymerase chain reaction (RT-qPCR) and western blot analysis were performed to evaluate the expressions of LINC00963, FoxO3a, TGF-β1, FN, GSH-PX, Bax, and Bcl-2. Measurement of changes in OS indexes including BUN, MDA, GSH-Px, SOD, and Na^+-K^+-ATP were conducted. Enzyme-linked immunosorbent assay (ELISA) was used to determine the levels of inflammatory factors including TNF-α, IL-6, ICAM-1 and FN. TUNEL staining was performed to evaluate cell apoptosis. ***Results:*** LINC00963 was highly expressed in CRF rats and FoxO3 was predicted and then verified as a target gene of LINC00963. FoxO3 gene participated in the FOXO signaling pathway. Compared with the blank and NC groups, there were significantly decreased expressions of LINC00963, TGF-β1, FN, and Bax in the si-LINC00963 group, while increased expressions of GSH-PX, FoxO3a, and Bcl-2. The vitality

Dr. Zhi-Kui Wang

Department of Nephrology, Linyi People's Hospital,
No. 27, Jiefang Road, Linyi 276003, Shandong Province (China)
Tel. +86-0539-8216273, E-Mail wangzhikui29@163.com

values of BUN and MDA in the si-LINC00963 group declined, while enzymatic activities of GSH-Px, SOD and Na^+-K^+-ATP elevated in comparison to the blank and NC groups. The levels of TNF-α, IL-6, ICAM-1 and FN, and cell apoptosis rate in the si-LINC00963 group decreased in comparison to the blank and NC groups. All the results in the si-LINC00963 group were opposite in the LINC00963 vector and si-FoxO3 groups. ***Conclusion:*** Taken together, we conclude that down-regulation of LINC00963 suppresses RIF and OS of CRF by activating the FoxO signaling pathway.

Introduction

Chronic renal failure (CRF) is defined as a glomerular filtration rate (GFR) below 15 ml/min per 1·73 m^2 for a long time [1]. CRF is a severe renal damage with a serious clinical symptom resulting from multiple predisposing factors, such as diabetes glomerulonephritis, and hypertension [2]. CRF is considered as one of the most significant public health problems, with accumulating rates of occurrence and development [3]. There are about 10% of the general adult population affected by CRF worldwide, which is often complicated by sepsis and cardiovascular disease [4]. Previous study has revealed that CRF is characterized by slowly progressive chronic renal interstitial fibrosis (RIF) and accompanied with increased oxidative stress (OS) that is already found in the early stage of renal disease [5]. Although a low protein diets is the effective treatment regimen for CRF, the side effects of this strategy cannot be ignored, such as a probable occurrence of proteinuria and functional impairment [6]. The underlying mechanisms and more effective therapies for CRF are still unknown.

Long non-coding RNAs (lncRNAs) are a group of non-protein-coding transcripts of over 200 nucleotides in length and they play crucial roles in tumor development and progression [7]. LncRNAs also have significant biological functions in modulating gene at transcriptional, post-transcriptional and chromosomal levels [8]. LncRNAs participate in physiological processes of cell-type determination and tissue homeostasis, and it has been proved that LINC00963 was involved in the prostate cancer transition from androgen-dependent to androgen-independent and metastasis via the epidermal growth factor receptor (EGFR) signaling pathway [9]. Moreover, a previous study has demonstrated that overexpression of lncRNA MEG3 promotes hepatic insulin resistance by upregulating forkhead box O (FoxO) 1 expression [10]. As a conserved subfamily of the forkhead transcription factors in evolution, FoxO transcription factors are characterized by the forkhead DNA-binding domain [11]. The FoxO subfamily of forkhead transcription factors consists of FoxO1 (FKHR), FoxO3 (FKHRL1), FoxO4 (AFX), and FoxO6, and the mediation of these transcription factors is determined by the availability of growth factors [12]. Furthermore, it has been reported that the FoxO transcription factors exert great effects on the regulation of cell growth, cell cycle, apoptosis, and the defense against oxidative stress (OS) [13, 14]. However, there are few articles that discuss the effects of lnc RNA and the FoxO signaling pathway on the CRF. Therefore, this study aims to explore the role of lncRNA LINC00936 in RIF and OS of CRF by regulating the FoxO signaling pathway, with the hope to find an efficacious therapy for CRF.

Materials and Methods

Ethics statement

Animal welfare and the relevant experiments were performed in compliance with the guide for the care and use of laboratory animals. The subject was approved by the ethics committee of Linyi People's Hospital in Shandong Province.

Bioinformatics prediction

Microarray data (GSE15072) and annotated probe files related to CRF were downloaded by retrieving Gene Expression Omnibus (GEO) database (http://www.ncbi.nlm.nih.gov/geo) and detected by Affymetrix

Human Genome U133 Plus 2.0 Array. Affy installation package of R software was used to process background correction and normalization of microarray data [15]. Then, linear model-empirical Bayesian statistics in the Limma installation package and the traditional *t*-test were combined for nonspecific filtration of gene expression data, thereby screening out differentially expressed lncRNA [16]. Multi Experiment Matrix (MEM, http://biit.cs.ut.ee/mem/) website was used to predict the differentially expressed lncRNA. MEM, as a web-based tool, is used to conduct co-expression queries on large collections of gene expression experiments. MEM has many publicly available gene expression datasets of distinct tissues, diseases and conditions, which are arranged by the species and microarray platform types [17]. The detailed instruction of MEM could refer to the website: https://biit.cs.ut.ee/beta_mem/help/mem_ismb_2009.pdf. WebGestalt database was used for Kyoto Encyclopedia of Genes and Genomes (KEGG) enrichment analysis of the target gene to identify the major biochemical metabolic pathways and signaling pathways involved [18].

Study subjects

A total of 60 Wistar male rats of half genders (aged 12 - 15 weeks old and weighted 200 - 250 g), were provided by Sichuan Jianyang Laboratory Animal Co., Ltd. All the rats were housed in separate cages according to gender with free access to food and water, and a 12-hour day/night cycle. Rats were reared at room temperature of 18 - 28°C, with relative humidity of 40% - 70%, and noise < 50 dB. The sixty rats were randomly assigned into the model (n = 50) and sham (n = 10) groups. The rat models of CRF (5/6Nx) were established as follows: the rats were anesthetized with 2% sodium pentobarbital, and fixed in the supination position on the operating table with conventional disinfection. The skin of the rats was opened along the white line in the middle of abdomen, and the abdominal cavity and left kidney were exposed. The renal capsular was cut with a blade to expose 2/3 of the kidney, which were cut off with a scalpel. Absorbable gelatin sponge was used in the incision for hemostasis, after which the renal capsular was stitched and the kidney was reset. Intraperitoneal injection of 3 μl of penicillin was performed, followed by stitched the incision. After three days, rats were anesthetized, the right abdominal cavity was opened and the right kidney was disassociated. Ligation of ureter and blood vessel of right kidney was conducted with stitch line, and the right kidney was removed. At 21 days after the second surgery, there were 3 rats died in the model group, while all rats in the sham group were alive. The weight of all rats was measured and urine volume within 24 h was collected to detect the urine protein. Ten rats (five rats in each group) were sacrificed. The criteria of the successful establishment [19] was as follows: the appetite reduction, loss of weight, increased water inflow, elevated urine volume, (3.3 ± 0.5) ml/rat, and increased urine protein (5.0 ± 0.5) mg/rat were found in the CRF rats. The rat scarification method was as follows: rats were intraperitoneally injected with 2% sodium pentobarbital and fixed in the supination position after anesthesia. Cardiac blood was extracted and mixed in the vacuum tube (Becton, Dickinson and Company, NJ, USA). Subsequently, the samples were centrifuged at 3000 r/min for 5 min, and the blood serum was preserved at -20° C. The skin in the abdomen was opened, and the left renal tissues were taken out. One part of them was preserved in liquid nitrogen, and the other part of them was fixed in 10% neutral formalin solution. After 24 h, the samples were dehydrated by gradient ethanol, and embedded in paraffin.

Plasmid construction and grouping

According to the mRNA sequences of LINC00963 and FoxO3 gene in Genebank, unrelated sequence, overexpression and interference fragments of LINC00963, and FoxO3 interference sequence synthesized by Shanghai Gene Chem Company (Shanghai, China) were designed sticking to the principle of RNA sequence design. All fragments were analyzed by Blast gene homology to identify the specificity. The amplified target fragments and the linearized plasmids (pcDNA3.1(-),Invitrogen Inc., Carlsbad, CA, USA) after enzyme digestion of BamH I and Hind III (Invitrogen Inc., Carlsbad, CA, USA) were connected at 16° C overnight under the effects of T4 DNA ligase. The connected products were transformed into DH5α competent cells (CB101, Tiangen Biotech Co, Ltd., Beijing, China). Next, the positive clones were selected and undergone sequence verification.

A total of 5 normal rats in the sham group and 30 rats in the model group were selected and assigned into the control (no treatment for normal rats), blank (no treatment for CRF rats), negative control (NC) (CRF rats injected with empty plasmid), LINC00963 vector (CRF rats injected with LINC00963 vector plasmid), si-LINC00963 (CRF rats injected with si-LINC00963 plasmid), si-FoxO3 (CRF rats injected with si-FoxO3 plasmid and inhibited FoxO signaling pathway), and si-LINC00963 + si-FoxO3 (CRF rats injected with

si-LINC00963 + si-FoxO3 plasmids) groups. Rats among seven groups were anesthetized with 2% sodium pentobarbital, and fixed in the supination position. The plasmids were injected through the caudal veins of rats. After three weeks, all rats were fasted for 12 h, and anesthetized with 2% sodium pentobarbital (50 mg/kg) via intraperitoneal injection. The left renal tissues were taken out, washed with phosphate buffered saline (PBS), fixed in 4% formaldehyde, embedded with paraffin, and prepared with sections.

Hematoxylin-eosin (HE) staining

Paraffin-embedded specimens of left renal tissues were randomly selected from five rats in the sham and model groups, and cut into 5-μm serial sections, which were spread at 45° C and gathered. After baked at 60° C for 1 h, the sections were dewaxed by xylene. Subsequently, the sections were stained with HE (Beijing Solarbio Science & Technology Co., Ltd., Beijing, China), dehydrated with gradient ethanol and cleared in xylene. After sealed with neutral balsam, the specimens were placed under the light microscope (XP-330, Shanghai Bing Yu Optical Instrument Co., Ltd., Shanghai, China) to observe the pathological changes of renal tissues of rats in the sham and model groups.

Immunohistochemistry

Paraffin-embedded left renal tissues of three rats were randomly selected from three rats in the sham and model groups, and were cut into 3 - 4 μm sections. The paraffin-embedded sections were immersed in 3% H_2O_2, xylene I and xylene II for 10 min, respectively, and in gradient ethanol of 100%, 95%, 80%, and 70% for 2 min successively. Next, the sections were washed with distilled water for twice, 5 min per time (placed on the shaking table). After immersed in 3% H_2O_2 for 10 min, the sections were washed with distilled water. The sections were received the antigen retrieval using a pressure cooker for 90 s, cooled at the room temperature, and washed with PBS. The sections were added with 5% bovine serum albumin (BSA) block solution and incubated at 37° C for 30 min. After that, the sections were added with rabbit anti-rat monoclonal antibody FoxO3 (ab16669, 1 : 100, Abcam, London, UK), and incubated at 4° C overnight. Subsequently, the IgG- horseradish peroxidase (HRP) biotinylated goat anti-rabbit secondary antibody (SE134, Beijing Solarbio Science & Technology Co., Ltd., Beijing, China) were added and incubated at 37° C for 30 min. The nucleuses were re-dyed by hematoxylin (C0105, Beyotime Biotechnology Co., Ltd., Shanghai, China) for 30 s, followed by developed by diaminobenzidine (DAB) (P0202, Beyotime Biotechnology Co., Ltd., Shanghai, China). After dehydration by hydrochloric acid and ethanol, the sections were cleared and mounted in gum. The sections were observed under the microscope and pictures were taken. The cytoplasm and cell membrane of positive cells were presented as brown. Five high power visual fields were randomly selected to observe the location of positive expression and percentage of the number of cells with positive expression of FOXO3 in the total number of cells. The experiment was repeated for three times.

Dual-luciferase reporter gene assay

To detect the connection of LINC00963 and Foxo3a, Foxo3a 3'-untranslated region (3'-UTR) wild type (Wt) and mutant type (Mut) luciferase reporter plasmids were constructed, named as Wt-Foxo3a-UTR and Mut-Foxo3a-UTR. Subsequently, two plasmids were respectively mixed with LINC00963 vector plasmids, si-LINC00963 plasmids and NC plasmids and then the mixtures were respectively co-transfected into HEK-293T cells (Shanghai Beinuo Biotech, Co., Ltd, Shanghai, China). After 24 h transfection, cells were collected, lysed, and centrifuged for 1 min at 12, 000 rpm with the supernatant collected. Each cell sample was added with 100 μL Firefly luciferase working fluid to detect Firefly luciferase activity. Similarly, each cell sample was added with 100 μL Renilla luciferase working fluid to detect Renilla luciferase activity. After that, the relative luciferase activity (RLA) was detected using Dual-Luciferase® Reporter Assay System (E1910, Madison, WI, USA). The RLA was determined by the ratio of Firefly luciferase activity and Renilla luciferase activity. The experiment was repeated for three times.

Reverse transcription quantitative polymerase chain reaction (RT-qPCR)

The left renal tissues preserved in liquid nitrogen and selected randomly from 21 rats among seven groups (3 rats in each group) were obtained. After grinding, 1 ml of Trizol reagent (Invitrogen, Carlsbad, CA, USA) was added to extract total RNA from tissues according to the instruction of Trizol kit. Ultraviolet (UV) spectrophotometer (UV1901, Shanghai Aucy Technology Instrument Co., Ltd., Shanghai, China) was used to evaluate the concentration and purity of RNA. The concentration of all samples with the purity of

A260/A280 = 1.8 - 2.0, was adjusted to 50 ng/μl. PrimeScriptTM RT reagent Kit (Takara RR047A, Beijing Zhijie Fangyuan Technology Co., Ltd., Beijing, China) was used to reversely transcribe total RNA into cDNA (50 ng/μl) with 10 μl of the reverse transcription system according to the instruction. The reaction conditions were as follows: reverse transcription reaction was performed at 37° C for 45 min (15 min × 3 times) and reverse transcriptase inactivation at 85° C for 5 s, after which the samples were preserved at -80° C. The Primer Premier 5.0 software was used to design primer sequences automatically, which were synthesized by TSINGKE Biological Technology Co., Ltd. (Beijing, China) (Table 1). The RT-qPCR experiment was undertaken using ABI 7900HT quantitative PCR System (ABI 7900, Shanghai PuDi Biotechnology Co., Ltd., Shanghai, China) with two-step method. The glyceraldehyde-3-phosphate dehydrogenase (GAPDH) was used as internal control. PCR reaction conditions were showed as follows: pre-denaturation at 95° C for 30 s, 40 cycles of denaturation at 95° C for 5 s, annealing at 95° C for 30 s, and final extension at 72° C for 15 s. The $2^{-\Delta\Delta Ct}$ method was applied to calculate the mRNA levels of LINC00963, FoxO3a, transforming growth factor β1 (TGF-β1), fibronectin (FN), glutathione peroxidase (GSH-PX), Bcl-2-associated X protein (Bax), and B-cell lymphoma-2 (Bcl-2) in the renal tissues of rats in the sham and model groups. Each gene in each sample was set for 3 wells. The experiment was repeated for three times. This method was also applicable for cell experiment.

Table 1. Primer sequence for RT-qPCR. Notes: RT-qPCR, reverse transcription quantitative polymerase chain reaction; FoxO3a, forkhead box O3a; LINC00963, long intergenic non-coding RNA 00963; TGF-β1, transforming growth factor β1; FN, fibronectin; GSH-PX, glutathione peroxidase; Bax, Bcl-2-associated X protein; Bcl-2, B-cell lymphoma-2; GAPDH, glyceraldehyde-3-phosphate dehydrogenase

Gene	Primer sequence
LINC00963	Forward: 5'-GGTAAATCGAGGCCCAGAGAT-3' Reverse: 5'-ACGTGGATGACAGCGTGTGA-3'
TGF-β1	Forward: 5'-GGCTGGTAAGGATGAAGG-3' Reverse: 5'-TGGAAGGAGGTCATACGG-3'
FN	Forward: 5'-CCATTCCTGCGCCAACCAATC-3' Reverse: 5'-GAGAGCTCCGGGCATTGTCGT-3'
GSH-PX,	Forward: 5'-GAGAAGTGCGAGGTGAATGGT-3' Reverse: 5'-GGGGGTTGCTAGACTGCTTGGAG-3'
FoxO3a	Forward: 5'-GCCACCCGAGTGTAACCAT-3' Reverse: 5'-TCCCTGGAGACCTGAAACC-3'
Bax	Forward: 5'-AAGCTGAGCGAGTGTCTCCGGCG-3' Reverse: 5'-GCCACAAAGATGGTCACTGTCTGCC-3'
Bcl-2	Forward: 5'-AGGATTGTGGCCTTCTTTGAG-3' Reverse: 5'-AGACAGCCAGGAGAAATCAAAC-3'
GAPDH	Forward: 5'-AGTCCACTG GCGTCTTCA-3' Reverse: 5'-GAGTC CTTCCACGATACCAA-3'

Western blot analysis

The left renal tissues preserved in liquid nitrogen and selected randomly from 21 rats among seven groups (3 rats in each group) were obtained, and were grinded to uniformly fine powder by grinder (M20, Shanghai Sheng Ke Instrument Equipment Co., Ltd., Shanghai, China). After washed with PBS for three times, samples were added with 100 ul of protein lysate (2 ug/ul), treated with ice reaction for 5 min, and centrifuged at 12000 r/min for 20 min. Total protein was extracted from nucleus and cytoplasm using Pierce Protein Isolation Kit (89826, Shanghai WEGENE Biotechnology Co., Ltd., Shanghai, China). Total protein concentration was determined using the bicinchoninic acid (BCA) reagent kit (P0012-1, Beyotime Biotechnology, Co., Ltd., Shanghai, China). The cells in the logarithmic growth phase were centrifuged at 3000 r/min at 4° C for 20 min, after which the supernatant was removed and packed cell volume (PCV) was estimated (cell volume after centrifugation). Cells were added with lysate (100 μl) and phosphatase inhibitor (1 μl) (1111111, Roche, Beijing Jiamay Biotechnology, Beijing, China) per 20 μl of PCV, treated with ice-cracking for 30 min, and centrifuged at 12000 r/min at low temperature for 10 min. The protein was extracted from nucleus and cytoplasm with the same way, and quantitative determination of which was conducted. A total of 50 μg of protein was taken out and immersed in sample buffer (2 × sodium dodecyl sulfate (SDS)). The samples were boiled at 100° C for 5 min. The proteins were separated by 10% SDS-polyacrylamide gel electrophoresis (PAGE) and then transferred to polyvinylidene fluoride (PVDF) membranes, which were blocked with 5% skimmed milk at room temperature for 1 h. After washed with PBS for 2 min, the diluted primary antibody rabbit anti-mouse FoxO3a (1: 1000, ab12162), TGF-β1 (1: 1000, ab131390), FN (1: 1000, ab156307), GSH-PX (1: 1000, ab40854), Bax (1: 1000, ab32503), Bcl-2 (1: 1000, ab119506), and GAPDH (1: 1000, ab8245) (Abcam, Shanghai, China) were added into PVDF membrane and incubated. After washed with Tris Buffered Saline with Tween-20 (TBST) for three times, the membrane

was incubated with goat anti-rabbit secondary antibody labeled by HRP (1 : 5000) for 1 h. Subsequently, the membrane was washed with TBST for three times, 5 min per time. The membrane was developed by electrochemiluminescence (ECL) reagent kit (10001, Beijing Keyushenlan Technology Co., Ltd., Beijing, China), exposed at X-ray, and photos were taken. Gel imaging analysis system (GelDoc XR+, Bio-Rad Laboratories Co., Ltd., Shanghai, China) was adopted to analyze the optical density (OD) value of developed band. The relative content of the sample protein was calculated as the mean OD value of samples divided by the mean OD value of corresponding internal control. The statistical analysis of the relative content of each sample protein was conducted. The experiment was repeated for three times. This method was also applicable for cell experiment.

The determination of changes in OS function

The left renal tissues selected randomly from three rats in each group were obtained. The specimens were washed with the normal saline, dried with filter paper, and placed in homogenizer. Next, sucrose (0.25 mol/l) and Tris buffer solution (0.01 mol/l) were added into to prepare the 10% tissue homogenates, which was centrifuged at 8000 r/min for 30 min. The supernatant was obtained to measure the activities and levels of OS markers in the cells, including blood urine nitrogen (BUN), glutathione peroxidase (GSH-PX), superoxide dismutase (SOD), malodialdehyde (MDA), and Na^+-K^+-ATP. BUN reagent kit (BU7120, Beijing Leadman Biochemical Technology Co., Ltd., Beijing, China), GSH-PX reagent kit (A005, Beijing Solarbio Science & Technology Co., Ltd., Beijing, China), SOD reagent kit (BC0170, Beijing Solarbio Science & Technology Co., Ltd., Beijing, China), MDA reagent kit (A003-1, Nanjing Jiancheng Bioengineering Institute, Nanjing, China), and Na^+-K^+-ATP reagent kit (QS1700, Shanghai Solarbio Bioscience & Technology Co., Ltd., Shanghai, China) were used. All determinations were undergone in strict accordance with the procedures of reagent kits. This method was also applicable for cell experiment.

Enzyme-linked immunosorbent assay (ELISA)

The left renal tissues preserved in liquid nitrogen and selected randomly from 14 rats among seven groups (2 rats in each group) were obtained. After grinding, the tissues were centrifuged and the supernatant was removed. Subsequently, ELISA was adopted to determine the levels of tumor necrosis factor-α (TNF-α), interleukin-6 (IL-6), intercellular adhesion molecule 1 (ICAM-1), and FN in renal tissues of rats. About 20 - 30 min before experiment, ELISA reagent kit (the number of TNF-α, IL-6, ICAM-1, and FN reagent kits were 69-25328, 69-40133, 69-30497 (Wuhan MSK Company, Wuhan, China), and BJ2809 (Shanghai Bang Jing Industrial Co., Ltd., Shanghai, China), and specimens were taken out from the refrigerator to balance to room temperature. The reagent kit and specimens were used at room temperature, and the solution was shaken slightly. A microplate reader (Multiskan GO, Thermo Fisher Scientific, CA, USA) was applied to analyze the OD value. The determination was in strict accordance with the instruction of reagent kits. The experiment was repeated for three times.

Terminal Deoxynucleotidyl Transferase (TdT)-mediated (dUTP) nick end-labeling (TUNEL) staining

Paraffin-embedded specimens of left renal tissues from three rats in each group were obtained. Subsequently, the specimens were dewaxed by xylene I and II for 10 min respectively, and immersed in gradient ethanol of 100%, 95%, 80% and 70% successively, each for 2 min, followed by washed with PBS for three times, 5 min per time. After that, the specimens were added into protease K working solution and incubated for 30 min, followed by washed with PBS for three times, 5 min per time. Then, the specimens were fixed in paraformaldehyde solution for 2 h. After washed with PBS for three times, 5 min per time, the specimens were immersed in 3% H_2O_2, dissolved in methanol, and closed at room temperature for 10 min. Next, the specimens were washed with PBS for three times, 5 min per time, and immersed in 20% sucrose phosphate buffer at 4° C overnight. On the following day, 20 μm serial transverse sections were prepared in the cryostat microtome at -22°C. Ten sections of each rat were stained by TUNEL according to the instruction of the TUNEL reagent kit purchased from Boehringer Mannheim GmbH, Mannheim, Germany. The cells with dark particles were considered as apoptotic cells under the light microscope (Leica DM4 P, Shanghai Mei Jing Electronic Co., Ltd., Shanghai, China). Ten high-power visual fields of sections in each group were selected. The apoptotic nucleus and the total number of cells were recorded, and the apoptotic index (AI) was calculated: AI = apoptotic cells/total cells. The value was calculated for three times and the mean value was taken.

Statistical analysis

The statistical analysis was conducted using SPSS 21.0 software (IBM Corp. Armonk, NY, USA). The measurement data were presented as the mean ± standard deviation (SD). Comparisons between two groups were analyzed using the *t* test. One-way analysis of variance (ANOVA) was used for comparisons among multiple groups. $p < 0.05$ was considered statistically significant.

Results

LINC00963 showed high expression in CRF and hemodialysis

According to the analysis of microarray data related to CRF (GSE15072), LINC00963 was highly expressed in CRF and hemodialysis, so LINC00963 was selected in this study (Fig. 1).

FoxO3 is predicted as a target gene of LINC00963

MEM was adopted to predict the target gene of LINC00963. A total of 13 out of the 200 predicted target genes were associated with signaling pathways, but only the FoxO signaling pathway was associated with the development of CRF. It was revealed that FoxO3 was a target gene of LINC00963 (Fig. 2A), and was also involved in the FoxO signaling pathway (Fig. 2B).

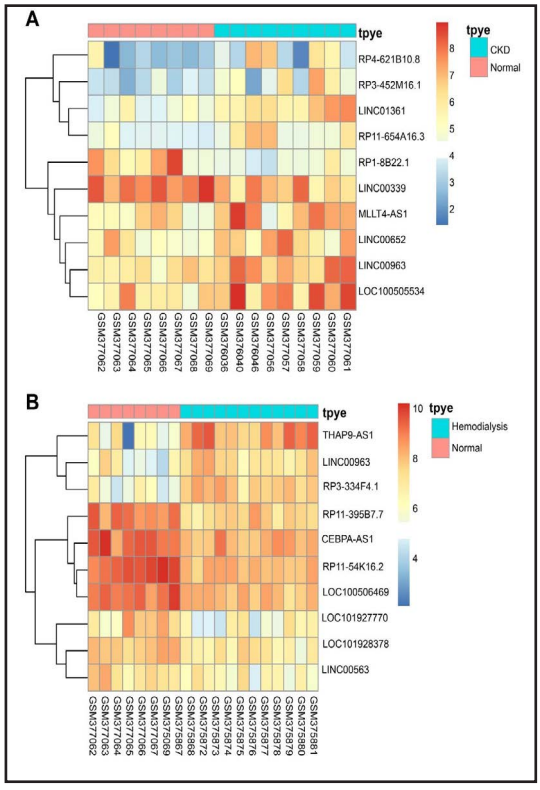

Fig. 1. LINC00963 showed high expression in CRF and hemodialysis according to microarray data (GSE15072) analysis (A, chronic kidney disease; B, hemodialysis) Notes: abscissa, sample number; ordinate, differential expressed gene; histogram in the upper right represents color gradation, and each rectangle represents an expression value of sample; red represents the high expression; green represents low expression; CRF, chronic renal failure.

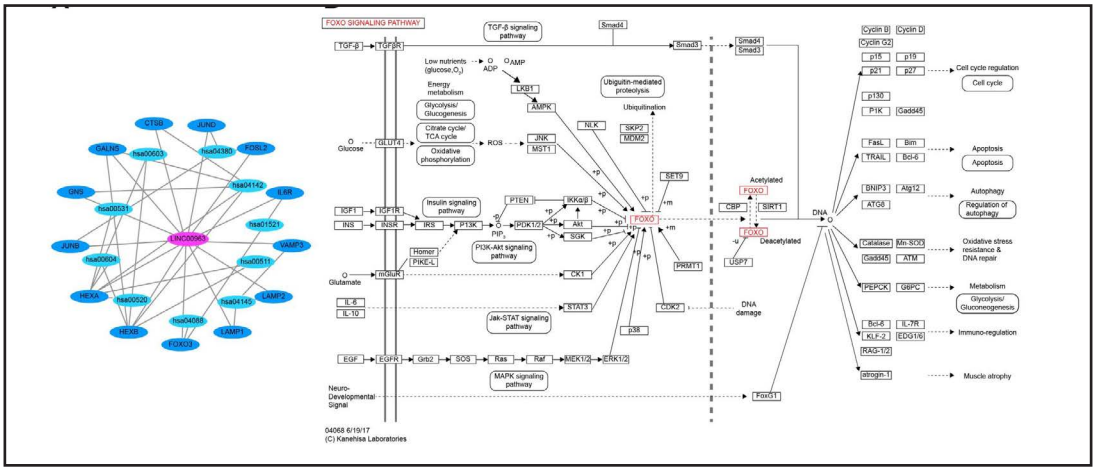

Fig. 2. FoxO3a was predicted to be the target gene of LINC00963 based on MEM analysis Note: A, prediction of the target gene of LINC00963 based on MEM analysis; B, the mechanism of FoxO3a involved in the FoxO signaling pathway based on KEGG enrichment analysis; FoxO3a, forkhead box O3a; LINC00963, long intergenic non-coding RNA 00963.

FoxO3a is verified to be a target gene of LINC00963

According to bioinformatics approach, FoXO3a sequences were found to specifically bind to LINC00963 sequences, FoxO3 served as a target gene of LINC00963 (Fig. 3A). The result of dual-luciferase reporter gene assay was shown in Fig. 3B, compared with the NC group, the Wt-FoXO3a-UTR + LINC00963 vector group showed decreased RLA, while the Wt-FoXO3a-UTR + siLINC00963 group showed increased RLA ($p < 0.05$). There was no difference in Mut-FoXO3a-UTR + LINC00963 vector and Mut-FoXO3a-UTR + si-LINC00963 groups ($p > 0.05$). All the results indicated that FoxO3a was a target gene of LINC00963.

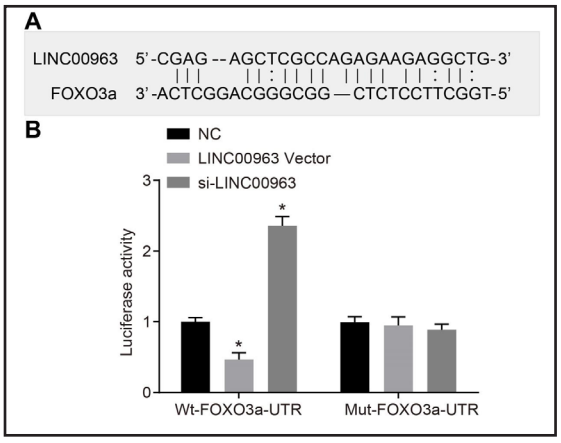

Fig. 3. FoxO3a was verified to be the target gene of LINC00963 Note: A, predicting LINC00963 binding sites on FoXO3a-UTR; B, histogram of RLA detected by dual luciferase reporter assay; *, p<0.05, compared with the NC group; NC, negative control; Wt, wild type; Mut, mutant; FoxO3a, forkhead box O3a; LINC00963, long intergenic non-coding RNA 00963.

CRF rat models is successfully established

Twenty-one days after surgery, the result of model establishment (Table 2) showed that 3 rats died in the model group, and 47 rat models of CRF were successfully established. All rats in the sham group were alive. Compared with the sham group, the weight of CRF rats in the model group significantly decreased, and the urine volume and urine protein significantly elevated 9.28 ± 1.19 mL and 8.53 ± 1.14 mg respectively within 24 h (all $p < 0.05$). It shows that the weight of CRF rats significantly decreased, and the urine volume and urine protein significantly elevated within 24 h.

Table 2. The determination results of physiological indexes of rats in the sham and model groups. Notes: OS, oxidative stress; BUN, blood urine nitrogen; GSH-PX, glutathione peroxidase; SOD, superoxide dismutase; MDA, methylene dioxyamphetamine

Group	Sham group (n = 10)	Model group (n = 47)	P
Weight (g)	271.33 ± 33.24	205.45 ± 23.48	< 0.001
Urine volume within 24 h (ml)	3.31 ± 0.52	9.28 ± 1.19	< 0.001
Urine protein (mg)	1.34 ± 0.21	8.53 ± 1.14	< 0.001

Table 3. The OS indexes of rats in the sham and model groups (n = 5)

Group	Sham group	Model group	P
GSH-PX (μmol/g)	273.50 ± 32.50	177.40 ± 19.56	< 0.001
SOD (U/mg)	1213.34 ± 134.56	544.98 ± 58.67	< 0.001
MDA (nmol/mg)	3.65 ± 0.43	12.87 ± 1.47	< 0.001
Na+-K+-ATP (μmol/g)	2106.70 ± 219.50	1283.50 ± 314.60	< 0.001
BUN (mmol/l)	6.74 ± 1.43	13.87 ± 1.12	< 0.001

Antioxidant resistance of CRF rats is weaker than normal rats

The activities of OS markers were measured to reflect the change of OS function in rats. The results (Table 3) showed that compared with the sham group, the vitality values of BUN and MDA in the model group significantly increased (2-4 folds that of the sham group), while activities of GSH-Px, SOD, and Na^+-K^+-ATP notably dropped to 177.40 ± 19.56 μmoL/g, 544.98 ± 58.67 U/mg and 1283.50 ± 314.60 μmol/g respectively (all $p < 0.05$), which indicated that the oxidation resistance of rats in the model group was

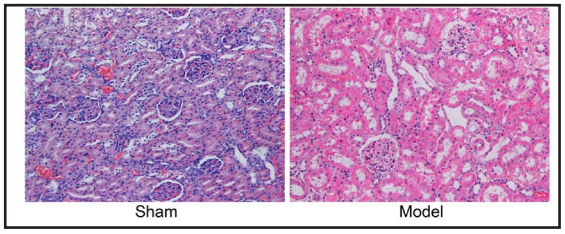

Fig. 4. Pathological morphological changes of left renal tissues of rats was more obvious in the model groups than in the sham group evaluated by HE staining (× 200).

weaker than that in the sham group.

CRF model rats exhibited obvious pathological changes

The results of HE staining in Fig. 4 showed that the size of renal tissues in the sham group was normal with darker color, and there were no changes in histology. The renal tissues in the model group showed an obvious increase, and focal fibrosis appeared with much invasion of lymph and monocytes, and nephron atrophy. The renal tubules were presented as cystic dilatation, and epithelial atrophy occurred.

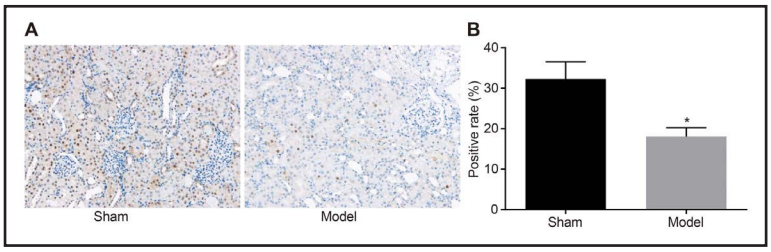

Fig. 5. Positive expression rate of FoxO3 protein in left renal tissues of rats was higher in the sham than in the model groups evaluated by immunohistochemistry Notes: A, the results of immunohistochemistry (× 200); B, histogram of positive expression rate of FoxO3 protein in the sham and model groups; *, p<0.05, compared with the sham group.

Positive expression rate of FoxO3 is lower in renal tissues of CRF rats

The results of immunohistochemistry were shown in the Fig. 5, FoxO3 protein was mainly expressed in the nucleus and its positive expression was stained with brownish-yellow. The brownish-yellow positive particles of left renal tissues in the sham group were more than that in the model group. FoxO3 protein positive expression rate was 32% in the sham group, while 18% in the model group. Compared with the sham group, the positive expression rate of FoxO3 protein in renal tissues of CRF rats was lower in the model group ($p < 0.05$). The results suggested that the a lower positive expression rate of FoxO3 protein was found in renal tissues of CRF rats.

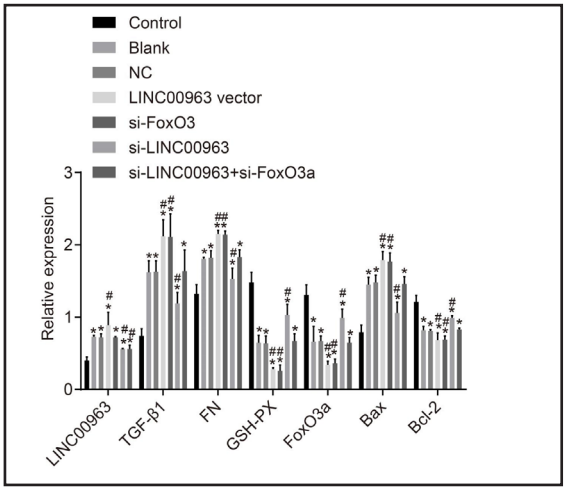

Fig. 6. LINC00963 inhibited related gene expressions in the FoxO signaling pathway detected by RT-qPCR Notes: *, p<0.05, compared with the control group; #, p<0.05, compared with the blank and NC groups; TGF-β1, transforming growth factor β1; FN, fibronectin; GSH-PX, glutathione peroxidase; Bax, Bcl-2-associated X protein; Bcl-2, B-cell lymphoma-2; FoxO3a, forkhead box O3a; LINC00963, long intergenic non-coding RNA 00963.

Lower LINC00963 expression promotes related gene expressions in the FoxO signaling pathway

The findings of RT-qPCR in the Fig. 6 showed that compared with the control group, the LINC00963 expression and mRNA expressions of TGF-β1, FN, and Bax in the rest six groups evidently increased, while the mRNA expressions of GSH-PX, FoxO3a, and Bcl-2 significantly decreased (all $p < 0.05$). In comparison to the blank and NC groups, the LINC00963 vector group showed an elevation in LINC00963 expression, and the LINC00963 vector and the si-FOXO3 groups showed increased mRNA expressions of TGF-β1, FN, and Bax, and decreased mRNA expressions of GSH-PX, FoxO3a, and Bcl-2 (all $p < 0.05$). The si-LINC00963 group showed decreased LINC00963 expression and mRNA expressions of, TGF-β1, FN, and Bax, and increased mRNA expressions of GSH-PX, FoxO3a, and Bcl-2 (all $p < 0.05$). The si-LINC00963 +

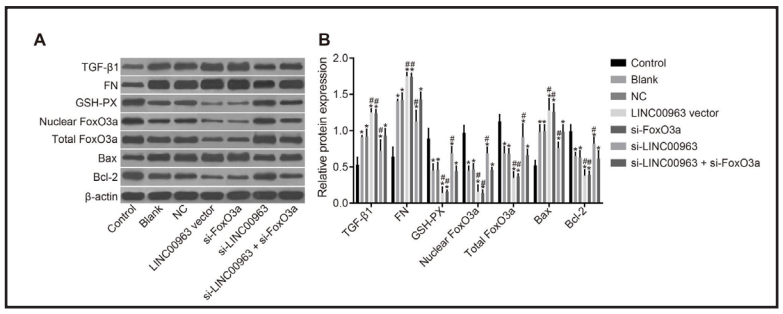

Fig. 7. LINC00963 inhibited related protein expressions in the FoxO signaling pathway detected by western blot assay Notes: A, protein bands for protein expressions in each group; B, histogram for protein expressions in each group; *, p<0.05, compared with the control group; #, p<0.05, compared with the blank and NC groups; TGF-β1, transforming growth factor β1; FN, fibronectin; GSH-PX, glutathione peroxidase; Bax, Bcl-2-associated X protein; Bcl-2, B-cell lymphoma-2; FoxO3a, forkhead box O3a; LINC00963, long intergenic non-coding RNA 00963.

si-FoxO3 group exhibited the down-regulated LINC00963 expression ($p < 0.05$), while no other obvious changes were found (all $p > 0.05$). All these results indicated that LINC00963 inhibits the activation of the FoxO signaling pathway, and lower expression of LINC00963 promoted the up-regulation of gene expressions related to the FoxO signaling pathway.

Table 4. The OS indexes of rats among seven groups (n = 5). Note: *,p < 0.05, compared with the control group; #, p < 0.05, compared with the blank and NC groups; NC, negative control; BUN, blood urine nitrogen; GSH-PX, glutathione peroxidase; SOD, superoxide dismutase; MDA, methylene dioxyamphetamine; OS, oxidative stress; FoxO3a, forkhead box O3a; LINC00963, long intergenic non-coding RNA 00963

Group	BUN (mmol/l)	GSH-PX (μmol/g)	SOD (U/mg)	MDA (nmol/mg)	Na^+-K^+-ATP (μmol/g)
Control	4.12 ± 0.76	273.25 ± 32.35	1213.34 ± 134.56	0.65 ± 0.04	2106.34 ± 219.35
Blank	15.35 ± 2.12*	177.34 ± 16.39*	588.22 ± 59.68*	2.74 ± 0.34*	1342.43 ± 121.32*
NC	16.05 ± 3.62*	172.15 ± 15.29*	573.62 ± 54.56*	2.62 ± 0.23*	1351.35 ± 123.32*
LINC00963 vector	28.79 ± 2.96#	113.55 ± 12.25*#	310.23 ± 141.42*#	4.78 ± 0.24*#	943.45 ± 101.34*#
si-FoxO3	29.65 ± 3.21*#	115.45 ± 11.29*#	293.42 ± 59.46*#	4.66 ± 0.33*#	937.54 ± 101.67*#
si-LINC00963	9.74 ± 2.22*#	231.35 ± 21.94*#	899.42 ± 59.46*#	1.55 ± 0.31*#	1679.65 ± 153.56*#
si-LINC + si-FoxO3	16.25 ± 3.25*	183.35 ± 24.93*	592.42 ± 55.36*#	2.84 ± 0.33*	1332.35 ± 134.25*

Table 5. The contents of TNF-α, IL-6, ICAM-1 and FN among seven groups. Note: *, p < 0.05, compared with the control group; #, p < 0.05, compared with the blank and NC groups; NC, negative control; FoxO3a, forkhead box O3a; LINC00963, long intergenic non-coding RNA 00963; TNF-α, tumor necrosis factor-α; IL-6, interleukin-6; ICAM-1, intercellular adhesion molecule 1; FN, fibronectin

Group	TNF-α (pg/ml)	IL-6 (pg/ml)	ICAM-1 (pg/ml)	FN (pg/ml)
Control	785.52 ± 81.24	535.53 ± 61.24	125.51 ± 12.82	158.53 ± 22.54
Blank	1875.56 ± 141.27*	975.5 ± 97.27*	256.54 ± 21.96*	328.57 ± 31.25*
NC	1861.58 ± 121.28*	985.58 ± 94.23*	253.54 ± 23.96*	329.54 ± 33.25*
LINC00963 vector	2512.38 ± 151.28*#	1222.34 ± 101.23*#	313.34 ± 41.24*#	401.33 ± 41.26*#
si-FoxO3	2493.2 ± 159.64*#	1253.22 ± 109.66*#	310.89 ± 29.64*#	403.20 ± 49.68*#
si-LINC00963	1329.2 ± 119.64*#	787.34 ± 59.65*#	179.24 ± 19.64*#	255.67 ± 29.6*#
si-LINC + si-FoxO3	1881.54 ± 131.23*	986.56 ± 95.27*	258.76 ± 22.97*	329.45 ± 35.28*

Lower LINC00963 expression promotes related protein expressions in the FoxO signaling pathway

The results of western blot analysis in Fig. 7 showed that compared with the control group, the protein expressions of TGF-β1, FN, and Bax in the rest six groups evidently increased, while the protein expressions of GSH-PX, total FoxO3a, nuclear FoxO3a, and Bcl-2 significantly decreased (all $p < 0.05$). In comparison to the blank and NC groups, the LINC00963 vector and the si-FOXO3 groups showed increased protein expressions of TGF-β1, FN, and Bax, and decreased protein expressions of GSH-PX, total FoxO3a, nuclear FoxO3a, and Bcl-2 (all $p < 0.05$), while the results in the si-LINC00963 group were opposite (all $p < 0.05$). The si-LINC00963 + si-FoxO3 group showed no other obvious changes in these protein expressions (all $p > 0.05$). All these results indicated that LINC00963 inhibits the activation of the FoxO signaling pathway, and lower expression of LINC00963 promoted the protein expressions related to the FoxO signaling pathway.

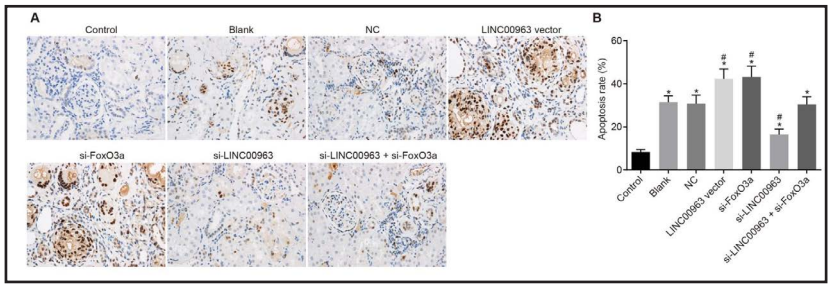

Fig. 8. LINC00963 promoted cell apoptosis detected by TUNAL staining Notes: A, the results of TUNEL staining (× 400); B, histogram for the apoptosis rate; *, p<0.05, compared with the control group; #, p<0.05, compared with the blank and NC groups; NC, negative control; FoxO3a, forkhead box O3a; LINC00963, long intergenic non-coding RNA 00963.

Lower LINC00963 expression improves OS function

The determination of changes in OS function was shown in the Table 4, compared with the control group, the vitality values of BUN and MDA in the rest six groups significantly increased, while the activities of GSH-Px, SOD, and Na^+-K^+-ATP notably decreased (all $p < 0.05$). Compared with the blank and NC groups, the LINC00963 vector and the si-FoxO3 groups showed the elevated vitality values of BUN and MDA, and reduced activities of GSH-Px, SOD, and Na^+-K^+-ATP, while the si-LINC00963 group showed the opposite results (all $p < 0.05$). No significant changes were found in the si-LINC00963 + si-FOXO3 group ($p > 0.05$). All these results indicated that overexpressed LINC00963 and under-expressed FoxO3 reduced OS function.

Lower LINC00963 expression reduces levels of TNF-α, IL-6, ICAM-1 and FN

The results of ELISA (Table 5) showed that the levels of TNF-α, IL-6, ICAM-1, and FN in the other groups notably increased in comparison to the control group (all $p < 0.05$). Compared with the blank and NC groups, the LINC00963 vector and the si-FoxO3 groups showed increased levels of TNF-α, IL-6, ICAM-1, and FN, while the results in the si-LINC00963 group were opposite (all $p < 0.05$). There were no obvious changes in the si-LINC00963 + si-FoxO3 group (all $p > 0.05$). All these results indicated that overexpressed LINC00963 and under-expressed FoxO3 promoted the expressions of inflammatory factors.

Lower LINC00963 expression reduces cell apoptosis rate of rat renal tissue

The results of TUNEL staining were presented in Fig. 8. The nucleuses of positive cell were presented as brownish-yellow. Compared with the control group, the apoptosis rate in the rest six groups was higher (all $p < 0.05$). The LINC00963 vector and the si-FoxO3 groups showed higher apoptosis rate and the si-LINC00963 group showed lower apoptosis rate in comparison to the blank and NC groups (all $p < 0.05$). The si-LINC00963 + si-FoxO3 group showed no evident changes (all $p > 0.05$). All these results indicated that overexpressed LINC00963 and under-expressed FoxO3 promote cell apoptosis rate of rat renal tissue.

Discussion

CRF remains a leading cause of death and loss of disability-adjusted life-years worldwide [20]. In recent years, lncRNA has become a potential therapy in diagnosing cancer disease, including renal cell carcinoma (RCC), and the biological markers in predicting the prognosis and the treatment for human disease [21]. In this study, we explored the effect of LINC00963 on RIF and OS of CRF through the FoxO signaling pathway, and found that down-regulation of LINC00963 suppressed the RIF and OS of CRF through the activation of the FoxO signaling pathway.

Initially, we found that the si-LINC00963 group showed significantly decreased expressions of LINC00963, TGF-β1 and FN in comparison to the blank and NC groups, which

indicated that lower LINC00963 expression activates the FoxO signaling pathway so as to inhibit RIF. In line with our study, a previous study has indicated that negative regulation of the FoxO signaling pathway activates the TGF-β1 and FN [22]. Another previous study has suggested that renal fibrosis is related to CRF progression and TGF-β1 is likely to accelerate this fibrosis [23]. In addition, FN, as a non-integral glycoprotein playing a role in regulation of fibroblasts and hepatocytes, exerts great effects on the regulation of cell migration, tissue repair, and cell adhesion [24]. Moreover, the elevated fibroblast growth factor (FGF)-23 serves as a risk factor for end-stage renal disease and for high mortality of CFR [25].

Additionally, compared with the blank and NC groups, the si-LINC00963 group showed decreased vitality values of BUN and MDA, levels of TNF-α, IL-6 and ICAM-1, while increased activities of GSH-Px, SOD and Na^+-K^+-ATP. It is known that OS and inflammation are major regulators of development of CRF [26]. Some previous studies have implied that both lncRNA and FoxO exert great effects on OS, for instance, up-regulation and down-regulation of lncRNA alter OS, and FoxO modulates the expression of several enzymes crucial for the cellular defense against OS [27, 28]. The overexpression of oxidative processes is involved in CRF patients and remains the significant factors for elevated morbidity and mortality in these patients [29]. Another research has showed that the balance between the production of reactive oxygen species (ROS) and the availability of antioxidant enzymes, such as SOD, BUN, MDA and GSH-Px, is consequently critical for avoiding the tissue damage induced by OS [30, 31]. GSH-Px, as one of the markers of oxidative stress, is highly expressed in RIF rats [32]. Moreover, FoxO3a has also been found to mitigate the oxidative threat posed by upregulating GSH-Px1 [33]. Wang et al. suggested that there was a positive feedback loop between inflammation and OS, and lncRNAs promoted tumorigenesis in cholangiocarcinoma (CCA) by activating this feedback loop [34]. In addition, CRF is correlated with elevation of inflammatory markers, which are observed at the severe stage of CRF and increases with progression of renal failure [35]. LncRNA CRNDE has been reported to correlate with immune process and cytokine response, which elevates the expressions of cytokines, including IL-6, CCL20, CXCL9, and TNFSF18 [36]. Furthermore, it has been proved that FoxO1 knockdown decreases expressions of inflammatory factors, including TNF-α, IL-1β and IL-18 [37], which is consistent with our findings.

Consequently, cell apoptosis rate in the si-LINC00963 group decreased with decreased Bax and increased Bcl-2 and FoxO3a expressions in comparison to the blank and NC groups. It has been reported that downregulation of lncRNA MALAT1 suppresses cardiomyocyte apoptosis [38], which is consistent with our results. FoxO3 was reported to participate in apoptosis resulting from infection with mycobacterium [39]. A previous study proved that FoxO3a suppresses apoptosis by induced HIF1 via induction of the transcription of lncRNA CITED2 [40]. From our study, we were able to demonstrate that lower expression of LINC00963 suppresses apoptosis by enhancing FoxO3 expression and activating the FoxO3 signaling pathway, hence to inhibit CRF.

In conclusion, lower expression of LINC00963 attenuated RIF and OS of CRF through activating the FoxO signaling pathway, which helps us to understand potential gene mechanisms of CRF and may provide new prognostic markers for the treatment of CRF in future. However, this study did not thoroughly investigate how LINC00963 affects activation of the FoxO signaling pathway as well as the potential mechanism in RIF and OS in CRF rats. Further studies are required to fully understand the specific mechanisms of LINC00963 targeting FoxO3 via the FoxO signaling pathway.

Acknowledgements

We would like to give our sincere appreciation to the reviewers for their helpful comments on this article.

Disclosure Statement

The authors have declared that no competing interests exist.

References

1 Ortiz A, Covic A, Fliser D, Fouque D, Goldsmith D, Kanbay M, Mallamaci F, Massy ZA, Rossignol P, Vanholder R, Wiecek A, Zoccali C, London GM, Board of the E-mWGoERAE: Epidemiology, contributors to, and clinical trials of mortality risk in chronic kidney failure. Lancet 2014;383:1831-1843.
2 Hu H, Xu S, Hu S, Xu W, Shui H: The clinical characteristics of posterior reversible encephalopathy syndrome in patients with chronic renal failure. Exp Ther Med 2017;14:881-887.
3 Zhao YY, Cheng XL, Wei F, Xiao XY, Sun WJ, Zhang Y, Lin RC: Serum metabonomics study of adenine-induced chronic renal failure in rats by ultra performance liquid chromatography coupled with quadrupole time-of-flight mass spectrometry. Biomarkers 2012;17:48-55.
4 Geng Z, Wei L, Zhang C, Yan X: Astragalus polysaccharide, a component of traditional Chinese medicine, inhibits muscle cell atrophy (cachexia) in an *in vivo* and *in vitro* rat model of chronic renal failure by activating the ubiquitin-proteasome pathway. Exp Ther Med 2017;14:91-96.
5 Walker RJ, Leader JP, Bedford JJ, Gobe G, Davis G, Vos FE, deJong S, Schollum JB: Chronic interstitial fibrosis in the rat kidney induced by long-term (6-mo) exposure to lithium. Am J Physiol Renal Physiol 2013;304:F300-307.
6 Piccoli GB, Leone F, Attini R, Parisi S, Fassio F, Deagostini MC, Ferraresi M, Clari R, Ghiotto S, Biolcati M, Giuffrida D, Rolfo A, Todros T: Association of low-protein supplemented diets with fetal growth in pregnant women with CKD. Clin J Am Soc Nephrol 2014;9:864-873.
7 Yang J, Lin J, Liu T, Chen T, Pan S, Huang W, Li S: Analysis of lncRNA expression profiles in non-small cell lung cancers (NSCLC) and their clinical subtypes. Lung Cancer 2014;85:110-115.
8 Cao W, Liu JN, Liu Z, Wang X, Han ZG, Ji T, Chen WT, Zou X: A three-lncRNA signature derived from the Atlas of ncRNA in cancer (TANRIC) database predicts the survival of patients with head and neck squamous cell carcinoma. Oral Oncol 2017;65:94-101.
9 Wang L, Han S, Jin G, Zhou X, Li M, Ying X, Wang L, Wu H, Zhu Q: Linc00963: a novel, long non-coding RNA involved in the transition of prostate cancer from androgen-dependence to androgen-independence. Int J Oncol 2014;44:2041-2049.
10 Zhu X, Wu YB, Zhou J, Kang DM: Upregulation of lncRNA MEG3 promotes hepatic insulin resistance via increasing FoxO1 expression. Biochem Biophys Res Commun 2016;469:319-325.
11 Ho KK, Myatt SS, Lam EW: Many forks in the path: cycling with FoxO. Oncogene 2008;27:2300-2311.
12 Hagenbuchner J, Kuznetsov A, Hermann M, Hausott B, Obexer P, Ausserlechner MJ: FOXO3-induced reactive oxygen species are regulated by BCL2L11 (Bim) and SESN3. J Cell Sci 2012;125:1191-1203.
13 Zhang X, Tang N, Hadden TJ, Rishi AK: Akt, FoxO and regulation of apoptosis. Biochim Biophys Acta 2011;1813:1978-1986.
14 Tzivion G, Dobson M, Ramakrishnan G: FoxO transcription factors; Regulation by AKT and 14-3-3 proteins. Biochim Biophys Acta 2011;1813:1938-1945.
15 Fujita A, Sato JR, Rodrigues Lde O, Ferreira CE, Sogayar MC: Evaluating different methods of microarray data normalization. BMC Bioinformatics 2006;7:469.
16 Smyth GK: Linear models and empirical bayes methods for assessing differential expression in microarray experiments. Stat Appl Genet Mol Biol 2004;3:Article3.
17 Adler P, Kolde R, Kull M, Tkachenko A, Peterson H, Reimand J, Vilo J: Mining for coexpression across hundreds of datasets using novel rank aggregation and visualization methods. Genome Biol 2009;10:R139.
18 Wang J, Duncan D, Shi Z, Zhang B: WEB-based GEne SeT AnaLysis Toolkit (WebGestalt): update 2013. Nucleic Acids Res 2013;41:W77-83.
19 Yang Y, Wei J, Huang X, Wu M, Lv Z, Tong P, Chang R: iTRAQ-Based Proteomics of Chronic Renal Failure Rats after FuShengong Decoction Treatment Reveals Haptoglobin and Alpha-1-Antitrypsin as Potential Biomarkers. Evid Based Complement Alternat Med 2017;2017:1480514.
20 Jha V, Garcia-Garcia G, Iseki K, Li Z, Naicker S, Plattner B, Saran R, Wang AY, Yang CW: Chronic kidney disease: global dimension and perspectives. Lancet 2013;382:260-272.

21 Xiong J, Liu Y, Jiang L, Zeng Y, Tang W: High expression of long non-coding RNA lncRNA-ATB is correlated with metastases and promotes cell migration and invasion in renal cell carcinoma. Jpn J Clin Oncol 2016;46:378-384.
22 Guo F, Wang Q, Zhou Y, Wu L, Ma X, Liu F, Huang F, Qin G: Lentiviral Vector-Mediated FoxO1 Overexpression Inhibits Extracellular Matrix Protein Secretion Under High Glucose Conditions in Mesangial Cells. J Cell Biochem 2016;117:74-83.
23 Lee SB, Kanasaki K, Kalluri R: Circulating TGF-beta1 as a reliable biomarker for chronic kidney disease progression in the African-American population. Kidney Int 2009;76:10-12.
24 Hymes JP, Klaenhammer TR: Stuck in the Middle: Fibronectin-Binding Proteins in Gram-Positive Bacteria. Front Microbiol 2016;7:1504.
25 Isakova T, Xie H, Yang W, Xie D, Anderson AH, Scialla J, Wahl P, Gutierrez OM, Steigerwalt S, He J, Schwartz S, Lo J, Ojo A, Sondheimer J, Hsu CY, Lash J, Leonard M, Kusek JW, Feldman HI, Wolf M, Chronic Renal Insufficiency Cohort Study G: Fibroblast growth factor 23 and risks of mortality and end-stage renal disease in patients with chronic kidney disease. JAMA 2011;305:2432-2439.
26 Kim HJ, Vaziri ND: Contribution of impaired Nrf2-Keap1 pathway to oxidative stress and inflammation in chronic renal failure. Am J Physiol Renal Physiol 2010;298:F662-671.
27 Tehrani SS, Karimian A, Parsian H, Majidinia M, Yousefi B: Multiple Functions of Long Non-Coding RNAs in Oxidative Stress, DNA Damage Response and Cancer Progression. J Cell Biochem 2017;10.1002/jcb.26217
28 Zheng X, Yang Z, Yue Z, Alvarez JD, Sehgal A: FOXO and insulin signaling regulate sensitivity of the circadian clock to oxidative stress. Proc Natl Acad Sci U S A 2007;104:15899-15904.
29 Popolo A, Autore G, Pinto A, Marzocco S: Oxidative stress in patients with cardiovascular disease and chronic renal failure. Free Radic Res 2013;47:346-356.
30 Giannakakis A, Zhang J, Jenjaroenpun P, Nama S, Zainolabidin N, Aau MY, Yarmishyn AA, Vaz C, Ivshina AV, Grinchuk OV, Voorhoeve M, Vardy LA, Sampath P, Kuznetsov VA, Kurochkin IV, Guccione E: Contrasting expression patterns of coding and noncoding parts of the human genome upon oxidative stress. Sci Rep 2015;5:9737.
31 Naguib YM, Azmy RM, Samaka RM, Salem MF: Pleurotus ostreatus opposes mitochondrial dysfunction and oxidative stress in acetaminophen-induced hepato-renal injury. BMC Complement Altern Med 2014;14:494.
32 Tao YY, Wang QL, Yuan JL, Shen L, Liu CH: Effects of vitamin E on mercuric chloride-induced renal interstitial fibrosis in rats and the antioxidative mechanism. Zhong Xi Yi Jie He Xue Bao 2011;9:201-208.
33 Kaushal N, Hegde S, Lumadue J, Paulson RF, Prabhu KS: The regulation of erythropoiesis by selenium in mice. Antioxid Redox Signal 2011;14:1403-1412.
34 Wang WT, Ye H, Wei PP, Han BW, He B, Chen ZH, Chen YQ: LncRNAs H19 and HULC, activated by oxidative stress, promote cell migration and invasion in cholangiocarcinoma through a ceRNA manner. J Hematol Oncol 2016;9:117.
35 Tbahriti HF, Meknassi D, Moussaoui R, Messaoudi A, Zemour L, Kaddous A, Bouchenak M, Mekki K: Inflammatory status in chronic renal failure: The role of homocysteinemia and pro-inflammatory cytokines. World J Nephrol 2013;2:31-37.
36 Li H, Li Q, Guo T, He W, Dong C, Wang Y: LncRNA CRNDE triggers inflammation through the TLR3-NF-kappaB-Cytokine signaling pathway. Tumour Biol 2017;39:1010428317703821.
37 Li Z, He Q, Zhai X, You Y, Li L, Hou Y, He F, Zhao Y, Zhao J: Foxo1-mediated inflammatory response after cerebral hemorrhage in rats. Neurosci Lett 2016;629:131-136.
38 Zhang M, Gu H, Xu W, Zhou X: Down-regulation of lncRNA MALAT1 reduces cardiomyocyte apoptosis and improves left ventricular function in diabetic rats. Int J Cardiol 2016;203:214-216.
39 Huang J, Jiao J, Xu W, Zhao H, Zhang C, Shi Y, Xiao Z: MiR-155 is upregulated in patients with active tuberculosis and inhibits apoptosis of monocytes by targeting FOXO3. Mol Med Rep 2015;12:7102-7108.
40 Bakker WJ, Harris IS, Mak TW: FOXO3a is activated in response to hypoxic stress and inhibits HIF1-induced apoptosis via regulation of CITED2. Mol Cell 2007;28:941-953.